An efficient Depalletizing System based on 2D Range Imagery

D.K. Katsoulas[1], D.I. Kosmopoulos[2]

[1] University of Freiburg, Institute for Pattern Recognition and Image Processing, Freiburg i.Br., D-79085

[2] National Technical University of Athens, Department of Electrical Engineering, Division of Computer Science, Athens, GR-157 73

Email: [1]dkats@informatik.uni-freiburg.de,[2]dkosmo@telecom.ntua.gr

Abstract

In this paper we propose an efficient approach towards the solution of the depalletizing problem, based on active vision. We describe a system comprising an industrial robot and a time of flight laser sensor, which performs the depalletizing task in real time, and independently of lighting conditions. In our case, the target objects are solid boxes of known identical dimensions, neatly layered but with arbitrary orientation within a layer, which are all placed on a platform. The layered structure of the target platform allows for two-dimensional imagery. The system locates the position of the boxes by tracking one of the corners they expose to the laser source. The system locates the desired corners by applying the scan line approximation technique [11], adapted to fit the needs of our application, to the two-dimensional input data. The advantages of our system over existing applications are its simplicity, robustness, speed and ease of installation.

1. Introduction

This paper addresses the depalletizing problem (or bin picking problem) in the context of which, a number of objects, of arbitrary dimensions, texture and type must be automatically located, grasped and transferred from a pallet, to a specific point defined by the user. The objects can be either placed on the pallet in a structured manner, for example, in the case of boxes, when they are placed on layers, or they can be jumbled. The requirement of a robust and generic automated depalletizing system stems primarily from the car and the food industries, where boxes and sacks of various dimensions, texture, and weight, either neatly placed, or jumbled, are laid on a pallet. By the term pallet we mean a rectangular platform like a table. A grouping of the configurations met at target pallets which are usually encountered at distribution centers or automobile industry factories has as follows: neatly placed identical sacks, jumbled identical sacks, neatly placed identical cardboard boxes, neatly placed identical boxlike objects, neatly placed boxlike objects or cardboard boxes or both, with varying dimensions, jumbled cardboard boxes, with varying dimensions. In this paper, we are addressing the third case, according to which neatly placed cardboard boxes are grasped and unloaded, but what is notable is that the technique used, could form a basis for the realization of a more general solution.

An automated system for depalletizing is of great importance because it undertakes a task that is very boring, strenuous and sometimes quite dangerous for humans. Furthermore, the robust and fast transfer of goods from an originating pallet to a target position (pallet, conveyor belt etc.) can accelerate significantly the logistics-processes in the industry and the warehouses. Thus much time and labor is saved and the costs are minimized.

1.1 Related Work

In general, the existing systems can be sorted in the following categories: systems incorporating no vision at all, and systems incorporating vision. The majority of the systems employed in industrial depalletizing applications so far, do not contain any vision modules. They usually employ preprogrammed gantry robots for bulk depalletizing tasks (e.g. [22], [23], [25], [26], [28]). Such systems may be much more effective in strictly controlled environments, (since they are fast and accurate), but they fail in adverse environments e.g. in a distribution center, where the pallet's position is not well-defined and the objects to be picked may be arbitrarily jumbled due to human intervention. In the initial attempts to use visual data, 2D techniques were employed, combined with additional sensors in the gripper to obtain the third dimension [14], [15]. These systems were limited to simple objects with special surface properties, e.g. identical cylindrical pieces of metal with a ground surface. Similar techniques are still used in the industry [24], where a feature-based approach identifies the objects to be picked by locating on them patterns such as letters or logos. These logo-tracking techniques are as well used in three-dimensional imagery [27]. The disadvantage of these methods is that they have all the problems of camera-based identification. The matching can fail in the case that the pattern does not appear, e.g. due to poor lighting conditions, reflections or dust. Furthermore, this method needs training for all patterns and is inappropriate in case that there is no obvious feature. Attempts incorporating range imagery seem much more promising. In [2] a structured light range sensor with additional sensors (force and proximity sensors) on the gripper were successfully employed, to deal with unloading piles of postal parcels with very good results. Even if the vision methods used did not allow for high accuracy, the idea of usage of range imagery and sensor fusion, resulted in a relatively efficient system. Nevertheless, the vision algorithm employed can only deal with planar objects. Its extension towards more complicated configurations is not straightforward. The recognition algorithms endorsed on the other hand, can take from 15 to 45 seconds to detect the position of only one graspable object at a time. Additionally, the disturbing of the pallet by the robot when the recognition system fails, may damage the target objects. The system of Vayda and Kak [20] deals with depalletizing of jumbled cylinders and parallelepipeds of unknown dimensions with the help of a range sensor. The authors attempt a complete scene understanding, via processes originating from artificial intelligence. According to these methods, size and pose estimation of target objects are facilitated by virtually extending their dimensions in the direction away from the sensor until they physically contact other objects in the scene The adoption of such methods results in an time-inefficient system, since the interpretation of complex scenes can take up to 20 minutes [2] in non-specialized hardware. The system closer to ours, is the one developed by Chen and Kak [5]. In both systems, a hypothesis generation for the existence of a target is based on Feature Sets (vertices in 3D in [5], corners in 2D here) detection. The hypothesis verification is performed by hardware in our case.

A direct comparison in grasping accuracy between the existing systems and ours is not possible, since no detailed accuracy measurements are provided by the systems' constructors. In the context of layered depalletizing of boxes, our framework surpasses all the existing systems as far as the speed, the ease of installation and the robustness are concerned because 2D - and thus simpler- image processing is applied.

A detailed description of our approach, as well as concrete experimental results follow in the subsequent paragraphs.

2. Depalletizing using a laser sensor

The system comprises a vision system that is responsible for the detection of the object's position and an industrial robot, which grasps the boxes. This system is based on one time-of-flight laser sensor, which is mounted on the robot's arm. The sensor is integrated on the tool, which performs the boxes' grasping (gripper) and is seamlessly attached to the robot's flange (figure 1). The laser sensor has specific advantages over cameras, since the measurements are not affected by environmental conditions like target objects' surface reflectance or lighting. The input data of the vision subsystem, is a set of two-dimensional points, which are defined as the intersection of the objects in front of the laser sensor, with the sensor's scanning plane, the range of which is adjustable. The integration of the laser sensor on the robot-hand allows for accurate data acquisition. Upon the input data, efficient algorithms that will be subsequently described are performed, which detect the boxes on the pallet. The system is characterized by speed, robustness, accuracy, low cost and ease of installation.

2.1 System configuration

A side view of the whole system and the pallet is presented in figure 1. The origin of the base coordinate system (B; $\mathbf{x}_b, \mathbf{y}_b, \mathbf{z}_b$) is located on the base of the robot. The relative position and orientation of (B; $\mathbf{x}_b, \mathbf{y}_b, \mathbf{z}_b$) to the world coordinate system (W; $\mathbf{x}_w, \mathbf{y}_w, \mathbf{z}_w$) is known a-priori [16]. We attach the coordinate systems (T; $\mathbf{x}_t, \mathbf{y}_t, \mathbf{z}_t$), (S; $\mathbf{x}_s, \mathbf{y}_s, \mathbf{z}_s$), (F; $\mathbf{x}_f, \mathbf{y}_f, \mathbf{z}_f$) to the robot tool (gripper) the sensor and the robot flange correspondingly as depicted in figure 1. We also attach the (C; $\mathbf{x}_c, \mathbf{y}_c, \mathbf{z}_c$) to the identified corner of the box so that $\mathbf{x}_c, \mathbf{y}_c$ are parallel to the box sides. The sensor provides the corner coordinates in the (S; $\mathbf{x}_s, \mathbf{y}_s, \mathbf{z}_s$), and the tool moves using the coordinates of the box centre transformed in (T; $\mathbf{x}_t, \mathbf{y}_t, \mathbf{z}_t$). The scanning plane is defined by the axes $\mathbf{x}_s, \mathbf{y}_s$.

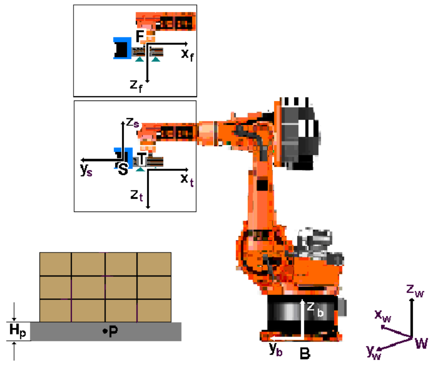

Figure 1. The world (W; $\mathbf{x}_w, \mathbf{y}_w, \mathbf{z}_w$), robot-base (B; $\mathbf{x}_b, \mathbf{y}_b, \mathbf{z}_b$), robot-tool (T; $\mathbf{x}_t, \mathbf{y}_t, \mathbf{z}_t$), robot-flange (F; $\mathbf{x}_f, \mathbf{y}_f, \mathbf{z}_f$) and sensor (S; $\mathbf{x}_s, \mathbf{y}_s, \mathbf{z}_s$) coordinate systems.

If ${}^{I}T_{J}$ denotes the homogeneous transform matrix from (I; $\mathbf{x}_i, \mathbf{y}_i, \mathbf{z}_i$), to (J; $\mathbf{x}_j, \mathbf{y}_j, \mathbf{z}_j$) then ${}^{T}T_{S}$ is obtained by calibration (see experimental results section), ${}^{S}T_{C}$ is calculated from the measurement data, and ${}^{T}T_{F}$ is given by the tool manufacturer.

The approximate position of the pallet P in (B; $\mathbf{x}_b, \mathbf{y}_b, \mathbf{z}_b$), the height of the pallet basis H_p, the layer height L_h and the maximum pallet height $Hh_{\max}$ are also required. These parameters are defined during the system's installation phase.

2.2 Operation

The flow diagram of the system is illustrated in figure 2. Initially the height of the upper layer of the heap is estimated. The sensor is positioned at distance T_h (figure 3b) from the ground where:

$$T_h = Hh_{\max} + H_p - L_h/2 \qquad (1)$$

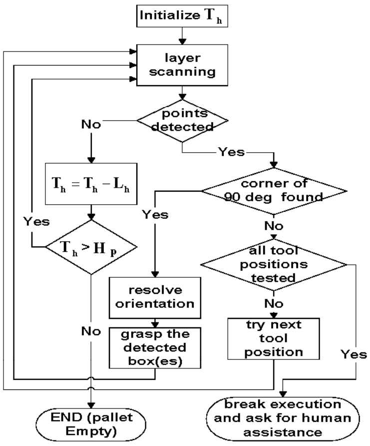

Figure 2. The flow diagram of the overall process

The scanning plane is parallel to the ground and $\mathbf{z}_s$ has the direction of $\mathbf{z}_b$. The vector $\mathbf{y}_s$ forms an angle of approximately 45 degrees with the pallet's side (figure 3a) in order to achieve higher accuracy (section 3) in the frequent case that the boxes are neatly placed on the layers of the pallet.

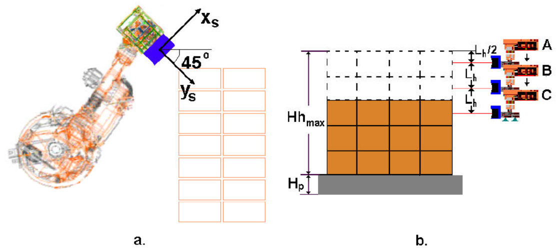

Figure 3 (a) The initial robot position – top view (b) The heap height estimation procedure – side view

The sensor performs a layer scanning and if no points are detected its height is decreased by L_h. The procedure is repeated until points are detected in the scanning area, e.g. at position C in figure 3b. From the acquired range data a scan line is derived and the box corners are extracted. In the event that no box corners could be extracted (figure 4a) the sensor is moved and rotated in order to acquire a better view of the boxes (figure 4b). Two such predefined movements are performed and if even now no corners can be detected, the system asks for human intervention. Otherwise the detected boxes are grasped and the layer unloading operation continues until the current layer is empty (no points appearing in the viewing range of the sensor). Then the tool goes down to the next layer and the process is repeated until the height of the tool is less than H_p (that is, when the pallet is empty).

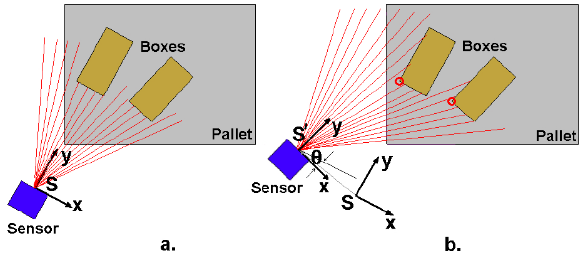

Figure 4 (a) The corner identification problem. (b) The sensor is moved and rotated and the corner(s) is (are) identified

Every time the sensor identifies a corner the grasping procedure is initiated. From the detected corner position, the centre of gravity of the box's upper surface G is calculated in (S; $\mathbf{x}_s, \mathbf{y}_s, \mathbf{z}_s$), and then it is transformed to (T; $\mathbf{x}_t, \mathbf{y}_t, \mathbf{z}_t$). The resulting frame is used to position the gripper onto G. If we attach the coordinate system (C; $\mathbf{x}_c, \mathbf{y}_c, \mathbf{z}_c$) to the identified corner of the box then ${}^{C}X_{G1}$ = (W/2, L/2, 0,1) (case A) or ${}^{C}X_{G2}$ = (L/2, W/2, 0,1) (case B) according to the orientation of the box (figure 5). In (T; $\mathbf{x}_t, \mathbf{y}_t, \mathbf{z}_t$) the point G will be given by:

$$ {}^{T}X_G = {}^{T}T_S \cdot {}^{S}T_C \cdot {}^{C}X_G \tag{2} $$

The orientation of the box is not known in advance and unfortunately it is very difficult to use the laser sensor for finding it, because in many cases the gap between the neighbouring boxes is 2-3mm (smaller than the sensor's resolution). Therefore, we send the gripper to the point where the gripper touches the topside of the box assuming that the orientation case is B (figure 5). If the actual case is B the gripper will sense low pressure and it is guided to ${}^{C}X_{G2}$. In the case A the gripper senses high pressure (no edge) and the gripper is sent to ${}^{C}X_{G1}$. Of course this solution is not optimal because much time is wasted in the attempt to find the orientation of the box. Later we will try to eliminate this procedure by employing a camera for this purpose.

The system in operation is displayed in figure 6.

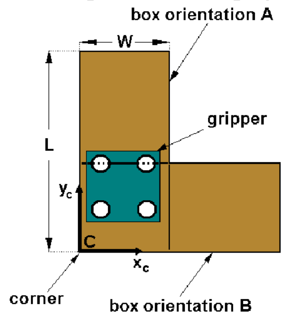

Figure 5. The gripper test position and the orientation cases in box-grasping

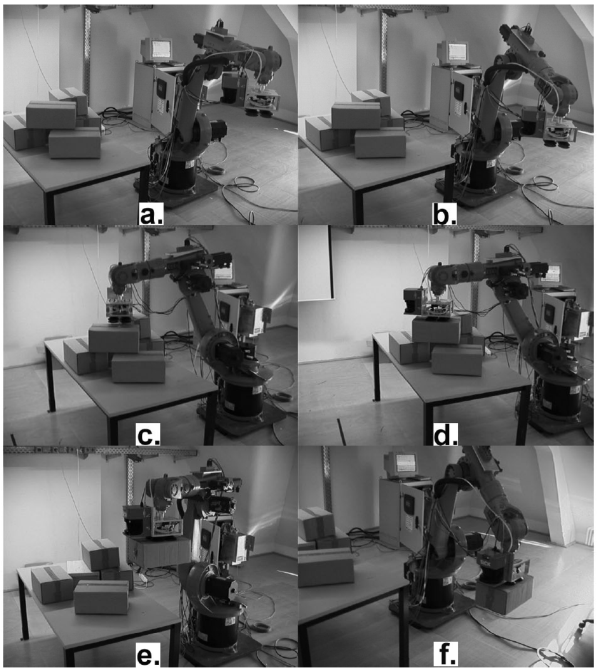

Figure 6 The system in operation: (a)-(b) heap height estimation (b) box localization (c) determination of orientation (d) box grasping (e) box picking (f) box placement.

2.3 Identification of box corners from 2D data

This is the core of the system. The input of the process is a set of planar points which comprise a two dimensional representation of the current layer of the pallet. The target of the process is the localization of the 90 degrees corner of the boxes to be grasped by the robot. In general terms we have to deal with the range image segmentation problem in two dimensions. From the vast literature having to do with range image segmentation based on 2D information (e.g. [1], [4], [7], [11], [21]), an algorithm should be selected, which should be efficient, accurate and able to deal with three-dimensional range data, when, in a future system, the objects on the pallet are not layered. The algorithm should have some sort of qualitative capabilities as well in order to detect the corners' size. An algorithm that satisfies the requirements stated above, is the one proposed by Jiang and Bunke [11], based on the Duda and Hart scan line splitting method [6], which detects and evaluates crease edges (discontinuities in range normal vectors.) and step edges (discontinuities in range values) in range data by using a scan line approximation technique. The particular algorithm was selected because of its simplicity and straight-forwardness, its potential to accurately deal, when combined with an edge grouping technique [18], with 3D configurations [9], [10], [11], [12], and finally its time-efficiency [17], which allows for rapid target detection when no image processing hardware is employed.

The scan line approximation algorithm splits the scan line to segments that can be accurately represented by functions. In figure 7a, a subset of a scan line is approximated with two curved segments namely $f_1(x), f_2(x)$.

From the edge points x_1 and x_2 the midpoint $\bar{x} = (x_1 + x_2)/2$ is extracted, with the help of which the jump and crease edge strengths are calculated as follows:

$$\text{Jump Edge Strength} = \left| f_1(\bar{x}) - f_2(\bar{x}) \right| \tag{3}$$

$$\text{Crease Edge Strength} = \cos^{-1}\left(\frac{(-f_1'(\bar{x}),1) \cdot (-f_2'(\bar{x}),1)}{\left\|(-f_1'(\bar{x}),1)\right\| \cdot \left\|(-f_2'(\bar{x}),1)\right\|} \right) \tag{4}$$

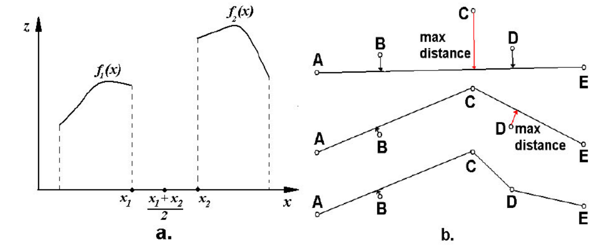

Figure 7 (a) Edge Strength Definition (b) The scan line splitting method

The accuracy in the edge strength value depends on the selected approximation functions. Our application induces the selection of linear functions. Thus, initially we represent each set of 2D points with a linear segment by means of the Duda and Hart [6] splitting method (figure 7b). If we suppose that our scan line comprises the points with labels A-E, a linear segment is initially estimated from the end points and the maximum distance of the line to every point of the scan line is calculated. If no point has a distance greater than T_{split} from the approximation curve, then the process stops for the particular scan line segment, since it is satisfactorily approximated. If the maximum distance is bigger than a predetermined threshold T_{split}, then the whole process is repeated recursively e.g. for the scan lines AC and CE.

Problems of the splitting method are the frequent over-segmentation of the scan line and the not optimal recovery of the real edge position [11]. The first problem can be solved with an appropriate selection of the threshold T_{split} in combination with a merge process. Over-segmentation problems are solved when the threshold T_{split} is increased. However, arbitrary increase in the value of T_{split} produces the under-segmentation phenomenon. In order to adjust the value of T_{split} we must have an a priori estimation of the noise level in the scan line. A solution to the problem is proposed in [3], according to which for every point of the scan line the previous and the next point are considered. Upon these points a straight-line segment is fitted. If the end points of the group modeled with the line, have an absolute difference in their y values bigger than two times the sensor's resolution R plus its random error E (both defined by the vendor) the point initially considered is regarded as belonging to a range discontinuity region and thus discarded. Otherwise, the approximation error is calculated. Given N_p the number of points of the smooth regions and $\in_{1,3}(p)$ the RMSE of the linear segment corresponding to the point p, the image's quality measure ρ is calculated as

$$\rho = \frac{1}{N_p} \sum_{P} \in_{1,3}(p) \qquad (5)$$

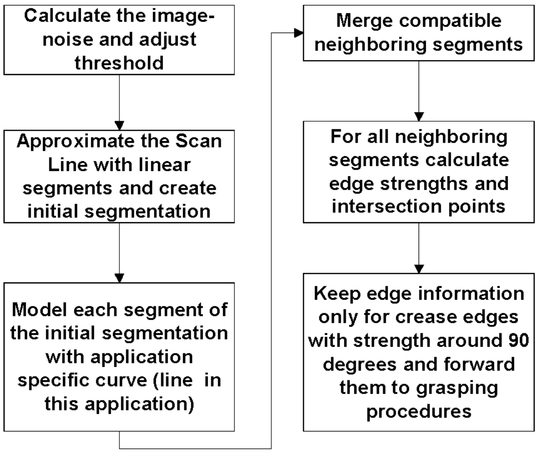

Figure 8. The layer scanning flow diagram

In our approach the threshold T_{split} was set to the value: $T_{split} = \rho + R$ where R is the resolution of the sensor. As mentioned, the second problem of this initial segmentation is that the edges generated do not correspond with accuracy to the real edge points. In order to realize higher accuracy, the initial segments produced are being again approximated. A least square fit is performed to the points comprising the segments originating from the splitting method. Due to the fact that, in some cases the over-segmentation problem could not be alleviated without a merging step, such a step is introduced by checking whether the angle of the normal vectors (AON), of least square modeled neighboring segments is lower than an input parameter.

Figure 8 describes in detail the adopted segmentation method. The corner position and orientation and the AON, are then forwarded to the grasping procedures, which move the gripper and grip the box(es).

3. Experimental results

Experimental setup As already mentioned, the system incorporates an industrial robot, namely the model KR 15/2 manufactured by KUKA GmbH, a square vacuum-gripper, which grips the boxes from their top side, and a time of flight laser sensor namely the model LMS200–30106, manufactured by SICK GmbH, with resolution 10mm, random error of 5mm and acquisition time 13ms. The sensor emits a beam, every f degrees, where $-\alpha \leq f \leq \alpha$ [19]. In our experiments, f=0.25 degrees and α=50 degrees. The system uses a Pentium PC (400 MHz, 256MB RAM), in which the vision software resides, as well as the necessary hardware needed for the grasping procedure operation. The system from the software point of view, comprises the vision module (implemented in C++), which accepts data from the laser sensor and calculates the position and orientation of the box(es), and the Robot controlling module (implemented in KUKA KRL), which requests correction frames from the vision module and moves the robot.

The inputs of the system during the initialization phase are the position of the center of the pallet P (figure 1) relative to the robot Base B coordinate system, the maximum heap height $Hh_{\max}$ (figure 3b), the dimensions H_p and L_h, the coordinate transformation matrices ${}^{T}T_S$, ${}^{T}T_F$, the sensor's resolution and its random error and finally the segments merging threshold. Only the latter should be extracted by experimentation, (in our experiments set to 2 degrees). A pallet of 1100mm×600mm was used with H_p=1000mm. The target objects were card boxes of 250mm×350mm with L_h =150mm. The sensor was placed 300 mm away from a corner of the pallet.

Calibration In order to calculate the transform matrix ${}^{T}T_S$ we executed a calibration procedure (offline). In this phase, we had to deal with the 3D – 3D absolute orientation problem, which is elegantly solved in [8]. According to this solution, when the coordinates of N 3D points relative both to the sensor and the tool reference frame are known, the transformation from the tool to the sensor can be determined by adopting a singular value decomposition approach. We used 5 3D points whose coordinates were known in both $(S; \mathbf{x}_s, \mathbf{y}_s, \mathbf{z}_s)$ and $(T; \mathbf{x}_t, \mathbf{y}_t, \mathbf{z}_t)$. In order to obtain these points, we used a solid box. The positions of the suction pads, which allow for gripping the box from the centre of its topside, were marked. We placed the box in various positions on the pallet and more specifically on the four corners and the center of it. For each position of the box, the position of one of the square box's corners (consequently the box's center) was calculated in $(S; \mathbf{x}_s, \mathbf{y}_s, \mathbf{z}_s)$. For each of the corners, we manually moved the robot's arm, in such a way that the suction pads fitted the marks on the topside of the target box. We noted the tool coordinates provided by the robot's console in $(T; \mathbf{x}_t, \mathbf{y}_t, \mathbf{z}_t)$ and in this respect we corresponded the coordinates of two coordinate systems. We have developed a software tool, which eases the above operation by helping the user to perform all the necessary actions. From the above, it is evident that the installation procedure is simple and can be executed within a reasonable amount of time. In all other systems known to the authors, the system's setup is much more time consuming and strenuous, since it requires sophisticated calibration procedures, training, or elaborate hardware installations on the ceiling of the installation site, or above the pallet.

Algorithm evaluation We verified the algorithm's performance regarding the accuracy and the speed. In order to estimate accuracy, a layer scanning was performed 50 times on a layer comprising up to 5 boxes. Many configurations of boxes were tried (some machine segmentation (MS) outputs are depicted in figure 9). Afterwards, two human operators examined the data. The operators identified the boxes, fitted lines to selected points on the sides of the boxes (they excluded noisy points) and calculated the corner's position, orientation and magnitude (ground truth–GT). The difference in measurements between MS and GT is displayed in (Table 1).

	Corner magnitude error (degrees)	Box orientation error (degrees)	Corner Position error (mm)		MS-GT corner distance (mm)
			X	Y	
Average	1.60	0.072	1.787	1.568	2.521
Standard deviation	1.80	0.137	1.191	1.257	1.531

Table 1. Segmentation algorithm's accuracy

The speed of the segmentation algorithm was estimated by executing the layer scanning operation 10000 times. 50 different boxes' configurations were tried, each one comprising up to five boxes. For each such configuration the system ran 200 times. The results are depicted in table 2.The time needed for a complete segmentation of the scan line, which comprises about 300 2D points is 1.56 ms. If we add the 13 ms of the scan line acquisition time to this quantity we come to the conclusion that the next graspable box can be detected in less than 15 ms, due to the fact that more than one boxes (1.8 on the average according to these experiments) can be detected in the scan line. This is significantly faster than any other solution to the problem proposed, up to our knowledge.

	Time (ms)/hit
Image Quality Calculation	0.41
Scan Line Splitting	0.79
Segment Approximation	0.10
Segments Merging	0.02
Edge Strength Calculation	0.24
Edge Detector (overall process)	**1.56**

Table 2. Processing time

Overall system's accuracy and robustness We placed the model box used in the calibration phase to various positions on the pallet (figure 10) with the depicted orientation. The position, and orientation of the box corner were measured in the tool coordinate system. Then we directed manually the tool so that the suction pads coincided with the marks on the box. The difference between the values observed on the robot's console and the calculated ones gave the system's overall accuracy measurements. For each position 20 measurements were executed.

The system proved its robustness by unloading the boxes every time for positions 1 to 17. In the cases of 16 and 17 the system was able to locate the box only after the automatic rotation and translation of the tool (due to the problem described in figure 4). Table 3 displays the results for positions 1 to 15. It is evident that as the exposed sides of the box face the laser beam with the same angle (45 degrees) the detection becomes more accurate. In the experiments conducted, in which the robot arm was executing linear movements with the maximum speed and acceleration [16], each box was grasped in less than 3 seconds, on the average.

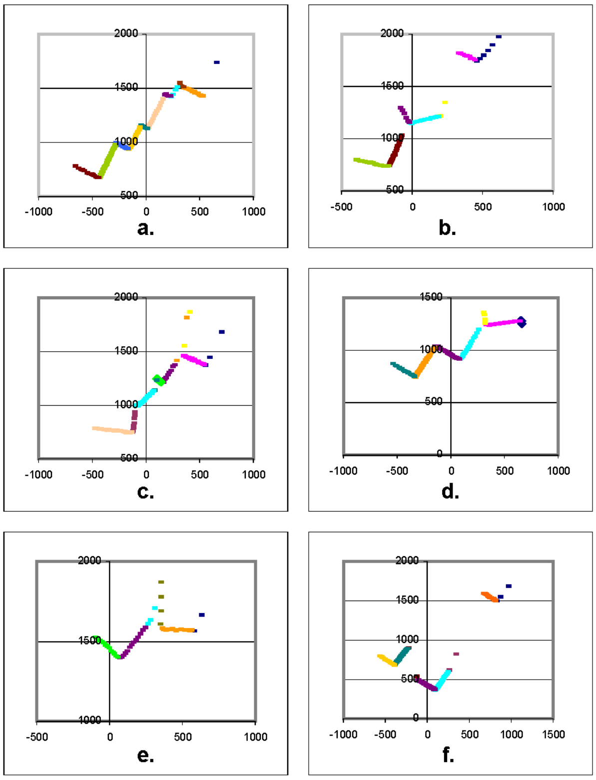

Figure 9 (a)-(f) The output of the segmentation procedure in some typical cases (all dimensions in millimeters).

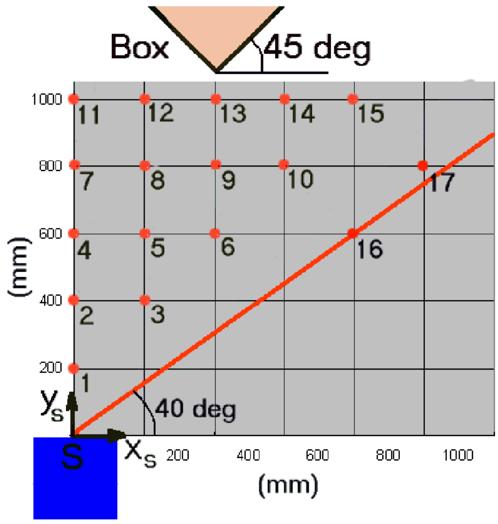

Figure 10 The measurement positions

	Position error (mm)		Orientation error (deg)	
Position	***mean***	***st. dev***	***Mean***	***st. dev***
1	14.64	1.66	0.45	0.90
2	14.50	1.85	1.59	1.08
3	15.55	1.03	2.20	1.11
4	14.72	2.48	1.70	1.33
5	15.53	1.92	1.88	0.94
6	15.84	1.55	1.06	0.58
7	15.09	2.95	0.42	0.57
8	15.30	3.06	2.80	1.48
9	16.22	4.57	2.55	1.50
10	18.32	5.23	2.95	1.77
11	14.86	1.62	2.05	1.71
12	16.35	2.44	1.39	1.14
13	16.57	3.42	2.40	1.34
14	17.55	4.41	2.81	1.84
15	18.25	5.35	2.88	1.80

Table 3 The system accuracy for the positions 1-15.

4. Conclusions and future work

In this paper a novel robotic system for depalletizing boxes was introduced and demonstrated. The task was executed using an industrial robot and a laser sensor for hand-eye coordination. The proposed solution to this problem is remarkably simple, fast and efficient. The boxes were always identified, independently of their appearance and of the illumination conditions. This is a major advantage against the camera-based solutions.

A variation of Jiang - Bunke range edge detection algorithm was employed and the corners were identified with mean accuracy better than 20mm in position and 5 degrees in orientation (mainly due to the systematic error of the sensor). This performance is sufficient for tasks like unloading a pallet to a conveyor belt but better accuracy would be probably desirable if the target position is another pallet. Therefore currently we try to implement a fine-localization procedure using a camera mounted on the robot's tool. The camera integration aims also to resolve the box orientation as mentioned in section 2.4.

In our future research we also plan to solve the problem of grasping piled boxes and piled sacks. Due to the fact that no layering exists, three-dimensional information should be extracted. Three-dimensional information will be obtained by collecting the scan lines acquired during a movement of the hand of the robot. Edge detection will be applied to the two dimensional scan lines and an edge grouping technique will be employed to extract desired feature sets. The algorithm presented, is able to deal not only with planar objects, but also with curved ones. According to this framework, the scan line approximation technique, should utilize curved functions [13] and not linear as in the application presented in this paper.

5. Acknowledgment

We gratefully thank Dr. Lambis Tassakos, INOS GmbH, for giving a hint to employ 2D techniques to deal with this problem and for supporting the first steps of this research. Many thanks are also due to Dr. Jens Schick and Dr Leonidas Bardis for their useful ideas and their overall support. We also wish to thank Professor Hans Burkhardt, University of Freiburg, Institute for Pattern Recognition and Image Processing and Dr. Costas Tzafestas for their fruitful comments on the manuscript.

References

[1] E. Al-Hujazi, A. Sood, "Range image segmentation with applications to robot bin-picking using vacuum gripper", IEEE transactions on Systems Man and Cybernetics 20(6), 1313-1325, 1990.

[2] A.J. Baerveldt, "Robust Singulation of Parcels with a Robot System using multiple sensors", Ph.D. Thesis, ETH No 10348, Swiss federal institute of technology, Zurich, 1993.

[3] P.J. Besl and R.C. Jain, "Segmentation Through Variable-Order Surface Fitting", IEEE Transactions on Pattern Analysis and Machine Intelligence, 10(2), 167–192, Feb. 1988.

[4] P. Boulanger et al., "Detection of depth and orientation discontinuities in range images using morphology", 10th International Conference in Pattern Recognition, B, 729-732, 1990.

[5] C.H.Chen and A.C.Kak, "A Robot Vision System for recognizing 3-D Objects in Low Order Polynomial Time", IEEE Transactions on SMC, Vol.19, No.6, 1989

[6] R.O. Duda, P.E. Hart, "Pattern Classification and Scene Analysis", Wiley, New York, 1972.

[7] S. Ghosal and R. Mehrota, "Detection of composite edges", IEEE Transactions on Image Processing 3(1), 14-25, 1994.

[8] Haralick et al., "Pose Estimation From Corresponding Point Data", IEEE Computer Society Workshop on Computer Vision, Miami, FL, pp. 258 –263, 1987.

[9] A. Hoover et al, "An experimental comparison of Range Image Segmentation Algorithms", IEEE Transactions on Pattern Analysis and Machine Intelligence, 18(7), 673-687, June 1996.

[10] X. Jiang, "Optimality analysis of edge detection algorithms for range images", Image Analysis and Processing, Lecture Notes in Computer Science, Springer, 1310, 182–189, 1997.

[11] X. Jiang, and H. Bunke, "Edge detection in range images based on scan line approximation", Computer Vision and Image Understanding, 73(2), 183–199, 1999.

[12] X.Y. Jiang et al., "A methodology for evaluating edge detection techniques for range images", 2nd Asian Conference on Computer Vision, Singapore, 2, 415-419, 1995.

[13] X.Y. Jiang et al., "High-level feature based range image segmentation", Image and Vision Computing 18(10) 817-822, 2000.

[14] R.B. Kelley, et al., "A robot system which acquires Cylindrical work-pieces from bins", IEEE Transactions. On Systems Man and Cybernetics, 12(2), March/April 1982.
[15] R.B. Kelly, "Heuristic Vision Algorithms for Bin-Picking", 14th Symposium on Industrial Robots, Gothenburg, Sweden, October, 1984.
[16] KUKA Roboter GmbH, KR 15/2 manual.
[17] E. Natonek, "Fast, Range Image Segmentation for Servicing Robots" IEEE International Conference on Robotics and Automation, 406-411, IEEE, May 1998.
[18] L. Thurfjell et al, "A new three-dimensional connected components labelling algorithm with simultaneous object feature extraction capability", Computer Vision Graphics and Image Processing, 51(4), July, 357-364, 1992.
[19] SICK GmbH, Measurement Software Tool (MST) technical description.
[20] A.J. Vayda and A.C. Kak, "A robot vision system for recognition of generic shaped objects", Computer Vision Graphics and Image Processing 54(1), 1-46, July 1991.
[21] M.A. Wani, B.G. Batchelor, "Edge region based segmentation of range images", IEEE Transactions on Pattern Analysis and Machine Intelligence 16(3), 314-319, 1994.
[22] www.abcpackaging.com/model108.html
[23] www.alvey.com/Products_Main_Sub_1.html
[24] www.automatedconcepts.com/home.html
[25] www.cat.it/english/index.htm
[26] www.iandh.com/pallet.html
[27] www.isra.de/frame/home_engl/produkt/index.html
[28] www.ocme.it/Maine.html